Research Square

Preprints are preliminary reports that have not undergone peer review.
They should not be considered conclusive, used to inform clinical practice,
or referenced by the media as validated information.

Synergistic effects of irrigation regime and straw crushing degree on nitrogen and phosphorus runoff and leaching in paddy fields

Jinhua Zhang
Hohai University
Han Han
Shihezi University
Xiaohui Xu
Hohai University
Xiangping Guo
xpguo@hhu.edu.cn

Hohai University
Jialiang Chen
Nanjing Gaochun District Water Affairs Bureau

Research Article

Keywords: Irrigation regime, Straw crushing degree, Nitrogen and phosphorus loss, Nitrogen and phosphorus leaching, Dissolved organic carbon

Posted Date: November 10th, 2026

DOI: https://doi.org/10.21203/rs.3.rs-11289093/v1

License: This work is licensed under a Creative Commons Attribution 4.0 International License.
Read Full License

Additional Declarations: No competing interests reported.

Abstract

To clarify the synergistic effects of irrigation regime and straw crushing degree on nitrogen and phosphorus loss and leaching in paddy fields and the DOC-mediated mechanism, based on a barrel experiment in 2023–2024, five treatments were set: conventional flooding without straw (CK), frequent and shallow irrigation + powdered/segmented straw (FSI + P/FSI + S), and controlled irrigation + powdered/segmented straw (CI + P/CI + S). Water dynamics and changes in nitrogen and phosphorus and DOC in surface water and seepage water were monitored. The results showed that controlled irrigation significantly reduced surface drainage, seepage, and TN and TP runoff loss and leaching flux by reducing irrigation frequency and water input; powdered straw was more conducive than segmented straw to enhancing nutrient retention and reducing mobile nitrogen and phosphorus concentrations, and its synergistic emission reduction effect with controlled irrigation was more prominent. DOC was extremely significantly positively correlated with NO_3^--N and TP leaching fluxes, and was an important carrier for the synergistic migration of carbon, nitrogen, and phosphorus. CI + P had the best comprehensive emission reduction effect, and it achieved optimal emission reduction through the synergistic pathway of water regulation–nutrient retention–DOC mediation, and can serve as a preferred integrated strategy for water conservation, nutrient loss mitigation, and straw resource utilization in paddy fields.

1. Introduction

In many rice-growing regions, paddy fields are a major contributor to non-point source pollution from agriculture. Nitrogen (N) and phosphorus (P) in surface water lost through runoff, and N and P in underground seepage water lost through leaching, are two key pathways leading to eutrophication of surrounding water bodies (Jiang et al., 2025). Consequently, mitigating nitrogen and phosphorus losses from rice paddies is critical for controlling non-point source pollution from agriculture and improving water resource use efficiency.

Irrigation regime is a core agronomic measure for regulating water status in paddy fields. Although traditional flooding irrigation ensures the water demand of rice, the deeper surface water layer increases the risk of N and P runoff loss (Li et al., 2018; Tan et al., 2013b). In contrast, water-saving irrigation modes represented by controlled irrigation (CI) break the long-term anaerobic state of soil through periodic drying and rewatering, and can effectively reduce runoff and percolation and lower the risk of nutrient loss. Tao (Tao et al., 2024) found that CI reduced percolation amount by 51.4% and runoff volume by 14.1% compared with conventional flooding irrigation, thereby reducing the risk of N and P leaching and runoff loss.

Returning straw to paddy fields represents a major exogenous carbon input and can raise soil organic carbon (SOC) levels, promote soil aggregation, and strengthen the soil's capacity to retain water and nutrients (Xia et al., 2018; Han et al., 2025). However, the effect of straw return on N and P loss has two sides. On the one hand, straw return can increase soil carbon-to-nitrogen ratio, promote microbial

immobilization of N, reduce soluble N concentration in surface water, and thus reduce the risk of nutrient loss (Zhang et al., 2025). Zhang (Zhang et al., 2021) found that under the same nitrogen application rate, double-season straw return reduced annual total N runoff loss by 23.5% compared with no straw return; Park (Park et al., 2021) confirmed that straw mulching return reduced carbon, nitrogen and phosphorus loss by 68%, 57% and 67%, respectively. However, when straw is returned without pretreatment, it can adversely affect tillage and rice root development, and may also provide suitable habitat for pathogens and insect eggs, leading to frequent occurrence of diseases and insect pests (Kerdraon et al., 2019; Shan et al., 2021). Straw crushing degree, as a key regulatory parameter of straw return, directly affects straw decomposition rate and nutrient release process (Yang et al., 2023; Iqbal et al., 2014), and may further change its regulatory effect on N and P loss in paddy fields. After straw crushing, the surface area increases, contact with microorganisms is more sufficient, and nutrients can be released faster (Tejada et al., 2014), which has greater potential in ensuring crop nutrient demand and reducing nutrient loss.

Among the constituent fractions of soil organic matter, dissolved organic carbon (DOC) is generally regarded as the most reactive. It not only participates in the carbon cycle, but also acts as an important carrier for N and P migration, affecting the dissolution, adsorption and leaching processes of N and P. Straw decomposition can continuously release DOC, change soil physicochemical properties and activate soil nutrients (Chen et al., 2023; Chen et al., 2024), while excessive DOC is easily accompanied by water percolation to carry N and P combinations and undergo vertical migration (Liu et al., 2025). However, under the combined regulation of irrigation regime and straw crushing degree, how DOC mediates the N and P leaching process, and whether it amplifies or weakens the synergistic regulatory effect of the two, is still unclear.

Irrigation regime and straw return have been extensively studied in relation to N and P loss in paddy fields, but the following three key issues have not yet been fully resolved: First, the interaction effect between irrigation regime and straw crushing degree is still unclear, and existing studies mostly focus on a single factor; Second, research on the differential effect of straw crushing degree is insufficient, and most studies use conventional segmented straw (2–10 cm), with less attention paid to the effect of powdered straw (< 2 mm); Third, there is a lack of systematic research on the DOC-mediated synergistic leaching mechanism of N and P, especially a lack of quantitative analysis of the relationship between DOC and N and P leaching. This study therefore aims to comprehensively examine how irrigation regime and straw crushing degree interact to influence water dynamics, the quality of surface water and subsurface percolation water, and nitrogen and phosphorus losses in paddy fields, reveal the DOC-mediated synergistic leaching mechanism of carbon, nitrogen and phosphorus, and screen the optimal combination mode. We hypothesize that: (1) CI directly reduces N and P loss fluxes by reducing water input; (2) powdered straw promotes soil nutrient retention more than segmented straw and reduces mobile nutrient concentrations; (3) the synergistic combination of CI and powdered straw indirectly reduces N and P leaching loss by inhibiting DOC leaching. These findings offer a scientific foundation and practical guidance for conserving irrigation water, reducing nutrient losses, utilizing straw resources, and mitigating non-point source pollution from agriculture in paddy fields.

2. Materials and methods

2.1 Experimental site

The experiment was conducted at the Water-Saving Park of Hohai University, Jiangning District, Nanjing City, Jiangsu Province (118°50'E, 31°57'N). The area lies within the middle and lower Yangtze River basin and is characterized by a typical rice–wheat rotation system. Data from the meteorological station near the park showed that from 2000 to 2022, the average annual temperature in this region was 14°C, and annual precipitation averaged 1 094 mm, the bulk of which fell during the rice-growing season. The soil texture is clay loam. The physicochemical properties of the soil surface layer (0–10 cm) measured 7 days before the start of the experiment were: SOC content 4.24 $g \cdot kg^{-1}$; total nitrogen content 0.36 $g \cdot kg^{-1}$; available phosphorus content 9.6 $mg \cdot kg^{-1}$; pH 7.2. Figure 1 presents the daily rainfall and mean air temperature recorded over the rice-growing period.

2.2 Experimental design and management

In 2018, a barrel experiment was set up in the Water-Saving Park, and the test soil was taken from the Water-Saving Park. The barrel used in the experiment was a plastic round barrel, the barrels were 80 cm in inner diameter and 85 cm in height, giving a horizontal cross-sectional area of 0.503 m^2. A cross-shaped water storage pipe (inner diameter 72 mm) was set at the bottom of the barrel. The upper end of the water storage pipe was vertically connected to a PVC drainage pipe with a height of 100 cm (outer diameter 70 mm, wall thickness 2 mm). A row of water collection holes with an inner diameter of 2 mm was set at the upper end of the water storage pipe, and the outside was tightly wrapped with a layer of non-woven fabric to prevent soil particles from entering the water storage pipe. Before soil filling, a 10 cm gravel cushion layer was laid at the bottom of the barrel to cover the cross-shaped water storage pipe. The air-dried and sieved soil was filled and compacted in 10 cm layers. The gravel cushion and soil layers together reached a depth of 70 cm, leaving 15 cm of water storage depth for rice irrigation and rainwater retention. The barrel experiment is shown in Fig. S1. Each experimental barrel was placed into the field soil to a depth of 70 cm, with its soil surface kept flush with the surrounding ground. This design could ensure that the crop canopy height in the barrel was consistent with that in the field, and the canopy light intensity, wind speed, temperature and humidity, and soil thermal conditions were all close to the real field environment, reducing the environmental deviation between the barrel experiment and the field. From 2018 to 2022, a preliminary experiment on water-saving irrigation was carried out. From 2023 to 2024, the combined experiment of water-saving irrigation and straw return was carried out. This study used a randomized block design. Two irrigation modes were set: frequent and shallow irrigation (FSI) and controlled irrigation (CI); two straw crushing degrees: powdered straw return and segmented straw. To evaluate the net effect of the combination modes compared with conventional management, conventional flooding without straw was set as the control group. A total of 5 experimental treatments were set, namely control (CK), frequent and shallow irrigation + powdered straw (FSI + P), frequent and

shallow irrigation + segmented straw (FSI + S), controlled irrigation + powdered straw (CI + P), and controlled irrigation + segmented straw (CI + S), with 3 replicates for each treatment.

The straw used in the experiment was wheat straw harvested from the previous season before rice transplanting, collected from this park, and uniformly air-dried after collection. Powdered straw was prepared by a grinder passing through a 2 mm sieve; segmented straw was cut into 2–5 cm lengths by a cutter. The measured carbon and nitrogen contents of the straw were: total carbon 446.69 $g \cdot kg^{-1}$, total nitrogen 7.18 $g \cdot kg^{-1}$, and C:N ratio 62:1. The straw return amount was set at 6 000 $kg \cdot hm^{-2}$ according to the local field recommended amount (Cong et al., 2020), and after conversion, the amount of straw applied to each experimental barrel was 300 g. All straw was returned by no-till mulching, that is, one day before rice transplanting each year, The prepared straw was applied uniformly to the soil surface at the predetermined rate.

The rice variety used in the experiment was Nanjing 46. In 2023, seedlings were raised on May 15, rice seedlings with three leaves and one heart were selected for transplanting on June 28, and harvest was on October 23; in 2024, seedlings were raised on May 17, transplanting was on June 27, and harvest was on October 30. Rice was planted at a field experimental planting density of 195 000 $plants \cdot hm^{-2}$, each barrel contained 12 hills, and each hill consisted of 3 plants. A day before rice transplanting, compound fertilizer (15% N, 15% P, and 15% K) was applied as basal fertilizer and incorporated into the tillage layer at 700 $kg \cdot hm^{-2}$. Urea (46% N) was used for both tillering and panicle fertilization, and were broadcast on the soil surface at a standard of 163 $kg \cdot hm^{-2}$. During the two-year experiment, the water regulation indicators, fertilizer application amount, fertilizer type and straw return amount were kept consistent. Weeding and insect control in the paddy field followed the conventional practices of the local experimental area. Water regulation is shown in Table S1, and the division of rice growth stages is shown in Table S2.

2.3 Collection and monitoring of surface water and deep percolation water

The collection of surface water aimed to capture the water quality status when surface runoff drainage actually occurred, and to accurately estimate the nitrogen and phosphorus loss loads under different combination modes. Due to the space limitation of the barrel experiment, the upper limit of rainwater storage for each treatment in this study was uniformly set at 50 mm in actual operation, as the trigger standard for artificial drainage. During the experiment, when the surface water layer in the experimental barrel exceeded 50 mm due to rainfall, artificial drainage was carried out to reduce the water layer to the upper irrigation limit of that treatment, and the drainage water quality indicators were measured. If there was no rainfall or the surface water layer did not exceed 50 mm, no drainage was carried out, and no surface water sample was collected. After the drainage of each experimental barrel was stirred evenly, 250 ml of water was taken, sampled three times, and the average value was taken.

The collection of deep percolation water differed from that of surface water. The collection of deep percolation water aimed to monitor the long-term intermittent effects of each treatment on soil profile water quality, and to evaluate the potential for vertical migration of nutrients to deep soil. This study adopted a regular fixed-frequency sampling strategy, taking water once every 5 days, to ensure that the soil was under free infiltration and not affected by rainfall or surface drainage events. Using the PVC drainage pipe and cross-shaped water storage pipe buried at a depth of 70 cm in the experimental barrel, a micro water pump with a 2 m long suction pipe was used during sampling to extract all the percolation water naturally accumulated in the water storage pipe since the last sampling was emptied through the PVC pipe. The water was collected in a graduated cylinder, and after recording the total drainage volume, a 250 ml subsample was taken and placed into a volumetric flask as one percolation water sample. After sampling was completed, the water storage pipe was completely emptied to prepare for the next accumulation of percolation water.

Drainage volume and percolation water volume recording: When surface water was drained, a graduated cylinder was used to record the surface drainage volume of each experimental barrel, and it was converted into drainage depth according to the bottom area of the experimental barrel. During percolation water collection, the total volume of percolation water extracted from the cross-shaped water storage pipe was recorded for subsequent calculation of leaching flux.

The collected water samples were brought back to the laboratory for measurement. TN was determined by alkaline potassium persulfate digestion ultraviolet spectrophotometry (Bronk et al., 2000); NH_4^+-N was determined by Nessler's reagent spectrophotometry (Skok et al., 2023); NO_3^--N was determined by hydrochloric acid acidified ultraviolet spectrophotometry (Huang et al., 2024); TP was determined by ammonium molybdate spectrophotometry (Murphy and Riley, 1962); DOC was filtered through a 0.45 μm microporous membrane and determined using a total organic carbon analyzer (TOC-L, Shimadzu, Japan).

Calculation of nutrient loss load and leaching flux. The apparent loss load of nitrogen and phosphorus in each drainage event was calculated according to Eq. (1):

$$L_i = C_i \times V_i \times 10^{-2} \quad (1)$$

Where: L_i is the apparent loss load of nitrogen and phosphorus in the i-th drainage event, kg·hm^{-2}; C_i is the nitrogen and phosphorus concentration in the i-th drainage event, mg·L^{-1}; V_i is the i-th drainage volume, mm. The total loss load is the sum of the loads of each drainage event. The leaching flux of deep percolation water was calculated by the same method, and the total leaching flux during the whole growth period is the sum of the leaching fluxes in each period. Because the percolation water collected each time was the natural accumulation amount within the interval period, the collected sample was a mixed sample within this period, which can reflect the average status of nitrogen and phosphorus concentrations in the percolation water during this period, rather than the instantaneous concentration.

2.4 Statistical analysis

Data organization was performed using Microsoft Excel 2021, while OriginPro 2025 was employed for visualizing water environment and soil nutrient indicators. Data normality (Shapiro-Wilk test) and variance homogeneity were assessed at $\alpha = 0.05$. One-way ANOVA was applied to compare treatment differences, and when significant, Tukey's HSD test was conducted for multiple comparisons.

3. Results

3.1 Water dynamics

From the total irrigation amount (Table S3), the total irrigation amount of different treatments in 2023 was in the order of CK > FSI > CI, and the corresponding total irrigation times were 12, 14 and 5, respectively. In 2024, a similar trend was observed. The total irrigation amount was highest in CK at 745.50 mm, followed by frequent and shallow irrigation at 656.04 mm, and lowest in controlled irrigation at 457.24 mm. The total irrigation times of CK and frequent and shallow irrigation were the same, both 22 times, and that of controlled irrigation was 10 times. Overall, the controlled irrigation mode reduced the total irrigation amount by reducing irrigation times, and saved 47.92% and 38.67% of water compared with CK in 2023 and 2024, respectively. For the frequent and shallow irrigation mode, the irrigation times in 2023 were 2 more than CK, and the irrigation times in 2024 were equal to CK, but it saved 12.50% and 12.00% of water compared with CK in 2023 and 2024, respectively, reflecting the irrigation characteristic of frequent and shallow irrigation with small amounts and multiple times.

The water-saving effect of CI was mainly concentrated in the tillering stage. During this period, the irrigation amount of CI decreased by 57.14–58.33% compared with CK, and the irrigation times decreased from 6–13 times in CK to 2–4 times. The jointing-booting stage is a critical period for rice water demand. CI maintained a relatively high irrigation amount during this period, reaching 228.62 mm in 2024, accounting for 50% of the total irrigation amount. No irrigation was carried out during the heading-flowering stage in CI, indicating that CI improved irrigation water use efficiency by compressing water supply in non-critical periods. Between the two years, the irrigation amount of each treatment in 2024 was higher than that in 2023, but the irrigation amount of CI treatment was always lower than that of CK and FSI, and the irrigation period was concentrated, showing good interannual stability.

CI treatment significantly reduced surface drainage volume (Table S4). In 2023, the total drainage volume of CI treatment decreased by 48.42–54.37% compared with CK and by 38.97–51.74% compared with FSI; in 2024, the total drainage volume of CI treatment decreased by 15.85–20.95% compared with CK and by 19.77–24.74% compared with FSI. Drainage events were mainly concentrated after fertilization and during heavy rainfall periods. The drainage volume of CI treatment in each drainage event was significantly lower than that of CK and FSI. Powdered straw showed an additional emission reduction effect under the CI mode. Compared with CI + S, the drainage volume of CI + P treatment

decreased by 11.53% in 2023 and 6.06% in 2024, indicating a synergistic emission reduction effect between CI and powdered straw.

Seepage water volume showed obvious seasonal variation, with July–August being the peak period of seepage, and then gradually decreased (Fig. 2). The seepage volume of CI was lower than that of CK and FSI in all periods. In the two years, CI seepage volume decreased by 24.29%–28.00% (2023) and 20.61%–23.00% (2024) compared with CK, and by 17.21%–21.00% (2023) and 9.36%–13.00% (2024) compared with FSI. Under the CI mode, powdered straw further reduced seepage volume: CI + P decreased seepage volume by 4.26% (2023) and 3.0% (2024) compared with CI + S, further confirming the synergistic effect of CI and powdered straw in reducing seepage (Table 1).

Table 1
Water input and output parameters under different treatments in 2023–2024

Year	Treatment	Precipitation/mm	Irrigation amount/mm	Surface runoff/mm	Seepage/mm
2023	CK	377.4	477.12	228.44	148.66
	FSI + P	377.4	417.48	193.09	136.18
	FSI + S	377.4	417.48	216.02	135.95
	CI + P	377.4	248.5	104.25	107.75
	CI + S	377.4	248.5	117.84	112.55
2024	CK	421.7	745.5	395.23	151.26
	FSI + P	421.7	656.04	415.15	132.61
	FSI + S	421.7	656.04	414.51	132.48
	CI + P	421.7	457.24	312.42	116.01
	CI + S	421.7	457.24	332.57	120.08

Note: CK: control; FSI + P: frequent and shallow irrigation + powdered straw; FSI + S: frequent and shallow irrigation + segmented straw; CI + P: controlled irrigation + powdered straw; CI + S: controlled irrigation + segmented straw.

3.2 Surface water quality and nitrogen and phosphorus runoff loss

TN and TP concentrations in surface water showed peaks after fertilization and then decreased rapidly (Fig. 3). In 2023, in the first drainage after basal fertilizer application, the TN concentration of CK was highest at 4.62–4.90 $mg \cdot L^{-1}$, and that of FSI + S was lowest at 0.87–0.96 $mg \cdot L^{-1}$. July 22 was the first drainage after tillering fertilizer application. The TN concentration of CK reached the highest peak during the whole growth period, with a fluctuation range of 4.62–4.90 $mg \cdot L^{-1}$. The TN concentration of CI + P was the lowest, decreased by 64.10% compared with CK, by 38.48%–45.31% compared with FSI, and by

7.25% compared with CI + S. On August 12 and after, the TN concentrations of all treatments decreased to below 1.30 $mg \cdot L^{-1}$. In 2024, June 30 was the first drainage 3 days after basal fertilizer application. The TN concentration of CK treatment was highest at 9.01–9.78 $mg \cdot L^{-1}$, and that of CI + S was lowest at 4.51–4.85 $mg \cdot L^{-1}$, decreased by 50.02% compared with CK. On July 8, the TN concentrations of all treatments decreased rapidly. Compared with the drainage on June 30, the largest decrease was in CI + P treatment, which decreased by 78.05%, followed by FSI + P treatment, with a decrease of 66.10%, and the smallest decrease was in CK, which decreased by only 34.33%. After July 14, the TN concentrations of all treatments decreased to below 1.0 $mg \cdot L^{-1}$.

In 2023, CK had the highest TP concentration in the first drainage, which was 2.20–2.56 $mg \cdot L^{-1}$. FSI + P and FSI + S were slightly lower than CK, decreased by 18.55% and 28.76% compared with CK, respectively, while CI + P and CI + S significantly reduced the initial TP concentration, decreased by 52.0% and 47.87% compared with CK, respectively. July 22 was the first drainage after tillering fertilizer application. The TP concentration of FSI was higher than that of CK. The TP concentrations of FSI + P and FSI + S increased by 17.95% and 15.32% compared with CK, respectively, while the TP concentration of CI was still lower than that of CK. The TP concentrations of CI + P and CI + S decreased by 38.98% and 19.35% compared with CK, respectively. In 2024, the overall peak TP concentration was lower than that in 2023 (Fig. 3). On June 30, the TP concentration of CK was 1.02 $mg \cdot L^{-1}$, and that of FSI + P was the lowest, decreased by 65.17% compared with CK and by 64.36% compared with FSI + S. Under the controlled irrigation mode, the TP concentrations of CI + P and CI + S treatments were both lower than that of CK, decreased by 57.92% and 31.23% compared with CK, respectively. On July 8, the TP concentration of CK increased to 1.16 $mg \cdot L^{-1}$, while the combination modes all showed a decreasing trend. The largest decrease was in FSI + P treatment, which decreased by 36.33%, and the smallest decrease was in CI + S treatment, which decreased by 20.76%. On July 14 and after, the TP concentrations of all treatments decreased to below 0.06 $mg \cdot L^{-1}$. It was noteworthy that under the controlled irrigation mode, the TP concentration of powdered straw treatment was lower than that of segmented straw treatment in both years, indicating that powdered straw had a certain promoting effect on reducing TP concentration in surface water.

NH_4^+-N in surface water is the main form of nitrogen loss. In 2023, CK had the highest NH_4^+-N concentration in the first drainage (Fig. S2), with a variation range of 4.26–4.39 $mg \cdot L^{-1}$, and it rose again to 2.35 $mg \cdot L^{-1}$ on July 22. CI + P and CI + S treatments decreased by 73.43% and 71.34% compared with CK, respectively. In 2024, all treatments reached a peak on June 30. CK was the highest at 6.26–6.70 $mg \cdot L^{-1}$, and CI + S was the lowest at 3.16–3.24 $mg \cdot L^{-1}$, decreased by 50.38% compared with CK. On July 8, all treatments decreased rapidly. On July 14 and after, the NH_4^+-N concentrations of all treatments were lower than 0.20 $mg \cdot L^{-1}$. The variation of NO_3^--N concentration was generally lower than that of NH_4^+-N. In 2023, CK had the highest NO_3^--N concentration in the first drainage, reaching 3.37–3.73 $mg \cdot L^{-1}$. FSI decreased by 46.90%–64.62% compared with CK, and CI decreased by 51.38%–54.11%

compared with CK. In 2024, the variation range of NO_3^--N concentration decreased significantly compared with 2023, showing a stronger nitrogen control ability.

Based on the concentration and drainage volume of each drainage event, the total apparent loss loads of nitrogen and phosphorus under different treatments were calculated (Table 2). The TN loss load of CI + P treatment was 1.32 kg·hm^{-2} in 2023, decreased by 75.87% compared with CK; it was 7.86 kg·hm^{-2} in 2024, decreased by 40.09% compared with CK. The TP loss load was 0.49 kg·hm^{-2} in 2023, decreased by 73.51% compared with CK; it was 0.60 kg·hm^{-2} in 2024, decreased by 64.07% compared with CK.

Table 2
Total apparent runoff losses of nitrogen and phosphorus in surface water under different treatments.

Year	Treatment	TN/(kg·hm^{-2})	TP/(kg·hm^{-2})
2023	CK	5.47 ± 0.100a	1.85 ± 0.093a
	FSI + P	3.04 ± 0.287b	1.36 ± 0.097b
	FSI + S	2.61 ± 0.106c	1.39 ± 0.042b
	CI + P	1.32 ± 0.059d	0.49 ± 0.027c
	CI + S	1.50 ± 0.085d	0.60 ± 0.026c
2024	CK	13.12 ± 0.303b	1.67 ± 0.085a
	FSI + P	13.92 ± 0.278a	0.65 ± 0.003c
	FSI + S	10.38 ± 0.185c	1.62 ± 0.071a
	CI + P	7.86 ± 0.154d	0.60 ± 0.075c
	CI + S	6.52 ± 0.115e	0.95 ± 0.049b

Note: CK: control; FSI + P: frequent and shallow irrigation + powdered straw; FSI + S: frequent and shallow irrigation + segmented straw; CI + P: controlled irrigation + powdered straw; CI + S: controlled irrigation + segmented straw. Values are expressed as means ± standard deviation (n = 3). Within a given year and column, means followed by different lowercase letters differ significantly among treatments ($P < 0.05$).

3.3 Seepage water quality and nitrogen and phosphorus leaching characteristics

TN concentration in seepage water was sensitive to fertilization, and obvious peaks appeared after three fertilizations during the rice growth period (Fig. 4). In 2023, CK reached the highest peak of the whole growth period after basal fertilizer, which was 4.75 mg·L^{-1}, and then decreased; after tillering fertilizer, a second peak appeared at 3.87–3.92 mg·L^{-1}; after panicle fertilizer, a third peak appeared at 3.46–3.64 mg·L^{-1}. The order of peaks in each period was CK > FSI > CI, and CI + P treatment was the lowest in each peak period. Compared with CK, TN concentration in CI treatment decreased by 10.55–15.37%, 10.98–

13.61% and 8.37–13.57% in the three peak periods, respectively. In 2024, the TN concentration dynamics were consistent with 2023, but the order of peaks changed. After basal fertilizer application in late June, TN concentration in FSI treatment decreased by 40.61–48.70% compared with CK, and the effect was better than that of CI, which was 9.13–13.51%; however, after tillering fertilizer application in late July, TN concentration in FSI treatment was higher than that in CK, and only CI + S treatment decreased by 13.41% compared with CK; after panicle fertilizer application in early September, TN concentrations in the combination modes were all lower than that in CK, and powdered straw treatment was better than segmented straw treatment, among which TN concentrations in CI + P and FSI + P treatments decreased by 1.82% and 14.27% compared with CI + S and FSI + S treatments, respectively. The concentration changes of NH_4^+-N and NO_3^--N in seepage water were consistent with the trend of TN (Fig.S3).

The change of TP concentration in seepage water was similar to that of nitrogen (Fig. 4). In 2023, TP concentration reached the largest peak of the year after basal fertilizer, with CK being the highest, and then decreased rapidly, decreasing to 0.081–0.121 $mg \cdot L^{-1}$ in mid-July. After tillering fertilizer, TP concentration rose again, and the order of peaks was CK > FSI+S > CI + S > FSI+P > CI + P. Under the same irrigation mode, TP concentration in powdered straw treatment was lower than that in segmented straw treatment. FSI + P and CI + P treatments decreased by 7.98% and 8.27% compared with FSI + S and CI + S treatments, respectively; under the same straw crushing degree, TP concentration in controlled irrigation mode was lower than that in frequent and shallow irrigation mode. CI + P and CI + S treatments decreased by 7.03% and 6.74% compared with FSI + P and FSI + S treatments, respectively. After panicle fertilizer, a small increase appeared, and only CI + P treatment had TP concentration lower than CK, with a decrease of 10.61%. In 2024, the overall peak TP concentration was lower than that in 2023. In late June, the peak of CK was the highest at 0.26 $mg \cdot L^{-1}$. Frequent and shallow irrigation treatments decreased by 39.16%–40.60% compared with CK, and controlled irrigation treatments decreased by 47.39%–50.00% compared with CK. After tillering fertilizer, the peaks of all treatments rose again. Under frequent and shallow irrigation mode, TP concentration in segmented straw treatment decreased by 6.42% compared with powdered straw treatment, and under controlled irrigation mode, TP concentration in powdered straw treatment decreased by 3.12% compared with segmented straw treatment. After panicle fertilizer application, a third peak appeared in early September, which was lower than the previous two peaks. The order of TP concentration was FSI + S > CI + S > CI + P > CK > FSI+P, among which only FSI + P treatment had TP concentration decreased by 2% compared with CK.

Based on seepage water volume and concentration, the N and P leaching fluxes under different treatments were calculated (Table 3). The TN leaching flux showed consistent variation patterns in 2023 and 2024, both CK > FSI > CI. In 2023, CK had the highest leaching flux at 2.65 $kg \cdot hm^{-2}$. Frequent and shallow irrigation treatments decreased by 13.28%–15.85% compared with CK, and controlled irrigation treatments decreased by 30.94%–40.00% compared with CK. Under the same irrigation mode, there was no significant difference between the two straw crushing degrees under FSI mode. Under CI mode, CI + P significantly decreased by 13.11% compared with CI + S ($P < 0.05$); under the same straw crushing degree, CI + P and CI + S significantly decreased by 28.70% and 20.09% compared with FSI + P and FSI +

S, respectively ($P < 0.05$). In 2024, TN leaching flux of FSI decreased by 25.93%–28.57% compared with CK, and that of CI decreased by 31.22%–37.04% compared with CK. Under the same irrigation mode, there was no significant difference between FSI + P and FSI + S, while CI + P significantly decreased by 8.46% compared with CI + S ($P < 0.05$); under the same straw crushing degree, CI + P and CI + S significantly decreased by 15.00% and 3.70% compared with FSI + P and FSI + S, respectively ($P < 0.05$). The leaching flux trends of NH_4^+-N and NO_3^--N were consistent with TN, both showing CK > FSI > CI in the two years. In 2023, NH_4^+-N leaching flux of CI decreased by 32.24–48.32% compared with CK, and NO_3^--N leaching flux decreased by 25.33–34.07% compared with CK; in 2024, they decreased by 31.81–45.49% and 36.86–45.97%, respectively. NH_4^+-N was the main form of nitrogen leaching, accounting for 35.30–47.75% of TN leaching flux in 2023 and 31.55–41.72% in 2024; NO_3^--N accounted for 37.55–45.59% and 12.27–15.46% of TN leaching flux in 2023 and 2024, respectively.

Table 3
Changes in carbon, nitrogen, and phosphorus leaching fluxes under different treatments in 2023–2024. (Unit: $kg \cdot hm^{-2}$)

Year	Treatment	TN	NH_4^+-N	NO_3^--N	TP
2023	CK	2.65 ± 0.03a	1.17 ± 0.07a	1.03 ± 0.02a	0.25 ± 0.004a
	FSI + P	2.23 ± 0.03b	0.90 ± 0.03c	0.88 ± 0.03b	0.22 ± 0.004c
	FSI + S	2.29 ± 0.05b	1.04 ± 0.05b	0.95 ± 0.03a	0.24 ± 0.009b
	CI + P	1.59 ± 0.03d	0.60 ± 0.04e	0.70 ± 0.01c	0.15 ± 0.008e
	CI + S	1.83 ± 0.05c	0.79 ± 0.05d	0.80 ± 0.02b	0.19 ± 0.006d
2024	CK	1.89 ± 0.06a	0.70 ± 0.02a	0.27 ± 0.009a	0.13 ± 0.003a
	FSI + P	1.40 ± 0.06b	0.56 ± 0.02b	0.21 ± 0.005b	0.10 ± 0.003b
	FSI + S	1.35 ± 0.02bc	0.48 ± 0.03c	0.19 ± 0.006c	0.10 ± 0.003b
	CI + P	1.19 ± 0.03e	0.38 ± 0.01d	0.15 ± 0.004e	0.07 ± 0.004d
	CI + S	1.30 ± 0.04d	0.48 ± 0.01c	0.17 ± 0.013d	0.08 ± 0.005c

Note: CK: control; FSI + P: frequent and shallow irrigation + powdered straw; FSI + S: frequent and shallow irrigation + segmented straw; CI + P: controlled irrigation + powdered straw; CI + S: controlled irrigation + segmented straw. Values are expressed as means ± standard deviation (n = 3). Within a given year and column, means followed by different lowercase letters differ significantly among treatments ($P < 0.05$).

TP leaching flux showed large differences between the two years, and decreased in 2024 relative to 2023, with an overall decrease of 46.05% (Table 3). In 2023, FSI + P and FSI + S significantly decreased by 13.42% and 6.06% compared with CK, respectively ($P < 0.05$); CI + P and CI + S significantly decreased by 39.74% and 24.70% compared with CK, respectively ($P < 0.05$). In 2024, the average TP leaching flux

of CK was 0.13 kg·hm^{-2}, that of FSI mode was 0.10 kg·hm^{-2}, significantly decreased by 25.66% compared with CK ($P < 0.05$), and that of CI mode was 0.08 kg·hm^{-2}, significantly decreased by 40.53% compared with CK ($P < 0.05$).

3.4 Correlation between DOC and nitrogen and phosphorus leaching

Within soil organic matter, dissolved organic carbon (DOC) is the most reactive fraction. When leached, it influences not only the carbon cycle but also the transport and transformation of N and P, functioning as a microbial carbon substrate and a nutrient carrier. The dynamics of DOC concentration in seepage water are shown in Fig. S4. To further reveal the role of DOC in N and P leaching, correlation analysis was conducted between DOC leaching flux and NO_3^--N and TP leaching fluxes, and the results are shown in Fig. 5. DOC and NO_3^--N were extremely significantly positively correlated in both years ($P < 0.001$), with $R^2 = 0.88$ in 2023 and $R^2 = 0.64$ in 2024; DOC and TP leaching flux showed a similar pattern, with $R^2 = 0.89$ ($P < 0.001$) in 2023 and $R^2 = 0.58$ ($P < 0.01$) in 2024.

Two-way ANOVA was performed to examine how irrigation regime, straw crushing degree, and their interaction influenced N and P leaching, thereby identifying the key controlling factors (Table 4). In 2023, irrigation regime and straw crushing degree had extremely significant effects on all indicators ($P < 0.001$); the interaction effect between irrigation regime and straw crushing degree was extremely significant only for TN ($P < 0.01$), and significant for TP ($P < 0.05$). In 2024, irrigation regime had extremely significant effects on all indicators ($P < 0.001$); straw crushing degree had no significant effect on all indicators ($P > 0.05$); the interaction between irrigation regime and straw crushing degree had extremely significant effects on DOC, NH_4^+-N and NO_3^--N ($P < 0.01$), and a significant effect on TN ($P < 0.05$).

Table 4
ANOVA results of carbon, nitrogen and phosphorus indicators.

Year	Factors	TN	NH_4^+-N	NO_3^--N	TP	DOC
2023	Irrigation regime	***	***	***	***	***
	Straw crushing degree	***	***	***	***	***
	Irrigation regime × Straw crushing degree	**	ns	ns	*	ns
2024	Irrigation regime	***	***	***	***	***
	Straw crushing degree	ns	ns	ns	ns	ns
	Irrigation regime × Straw crushing degree	*	***	**	ns	***

Note: Significance * $P < 0.05$; ** $P < 0.01$; *** $P < 0.001$; ns = not significant ($P \geq 0.05$).

4. Discussion

4.1 Regulation mechanism of irrigation regime and straw crushing degree on water dynamics in paddy fields

Paddy field water dynamics is a core carrier for regulating pollutant migration and transformation, and its changes play a decisive role in surface water runoff loss and underground seepage water leaching in paddy fields. The interaction between irrigation regime and straw crushing degree achieves precise regulation of paddy field water cycle by changing the processes of water input, output and transformation in paddy fields (Li et al., 2025). The results of this study showed that the controlled irrigation mode significantly reduced total irrigation amount, surface drainage volume and underground seepage water volume by optimizing irrigation timing and reducing irrigation frequency. This is consistent with the conclusion in current studies that the controlled irrigation mode reduces water consumption in paddy fields by supplying water during critical periods of rice and controlling water during non-critical periods (Amin et al., 2021). This study further found that the water-saving effect of CI mode was stable in the two-year experiment. In 2024, due to uneven rainfall distribution, there was very little rainfall during the tillering stage and jointing-booting stage of rice, resulting in significantly higher irrigation amounts for all treatments than in 2023, but the water-saving amplitude of CI mode compared with FSI mode and CK still maintained a relatively high level, indicating that this mode has strong adaptability to climate change.

The regulation of straw crushing degree on paddy field water dynamics is mainly reflected in water retention and seepage inhibition, and it can have significant interaction with different irrigation modes. In this study, the surface drainage volume and seepage water volume of powdered straw showed a small decrease relative to segmented straw, especially under CI mode, where this difference was more significant. This may be related to the denser mulch layer of powdered straw and its stronger water-holding capacity, which can form a more effective physical barrier and thus slow down soil water infiltration (Zhang et al., 2020). Under the FSI mode, there was no significant difference in seepage water volume between the two straw crushing degrees, possibly because the surface water layer was always maintained in the FSI paddy field, and soil water infiltration mainly depended on soil saturated hydraulic conductivity (Tan et al., 2013a), and the improvement of soil pore structure by straw crushing degree was weakened. This interaction effect provides a precise basis for the optimization of straw return technology under irrigation modes.

4.2 Synergistic regulation pattern and intrinsic mechanism of carbon, nitrogen and phosphorus migration and loss in paddy fields

N is the main pollutant of non-point source pollution in paddy fields. Its migration pathways are mainly surface water loss and underground seepage water leaching in paddy fields. The interaction between irrigation regime and straw crushing degree can achieve effective control of nitrogen loss by regulating N transformation, adsorption and migration processes (Han et al., 2025). The results of this study showed

that both the apparent loss load of N in surface water and the N leaching flux in groundwater followed the pattern of CK > FSI > CI, this finding agrees with earlier reports that N leaching is lower under water-saving irrigation (Gbedourorou et al., 2025; Qi et al., 2023; Huang et al., 2024). This study further quantified the emission reduction amplitude under the interaction of irrigation regime and straw crushing degree, and found that the TN leaching flux and apparent loss load of CI + P were significantly reduced compared with CK, and this emission reduction effect remained stable in the two-year experiment, indicating that the combination of CI and powdered straw is reliable for controlling N loss in paddy fields.

The migration and loss characteristics of different nitrogen forms also showed significant differences. NH_4^+-N is the main form of surface water loss, while NO_3^--N is the main form of underground seepage water leaching. This difference is related to the chemical characteristics of the two nitrogen forms. NH_4^+-N is easily adsorbed by soil colloids and has weak mobility (Li et al., 2023), and its loss is mainly related to surface water runoff; NO_3^--N is not easily adsorbed by soil, has strong mobility, and is easily lost with underground seepage water leaching (Wen et al., 2024). In this study, the inhibitory effect of CI on NO_3^--N leaching was significantly higher than that on NH_4^+-N, possibly because the CI reduced the total amount of underground seepage water and reduced the carrier for NO_3^--N migration; in addition, by regulating soil water status, the soil was in an alternating dry and wet state, which promoted the denitrification of NO_3^--N and reduced its accumulation in the soil profile (Jin et al., 2020). The effect of straw crushing degree on N loss was regulated by irrigation mode. Under FSI, there was no significant difference in N loss between the two straw crushing degrees; under CI, the N loss of powdered straw was significantly lower than that of segmented straw, which may be related to the faster decomposition of powdered straw and more sufficient contact with soil, thereby enhancing soil nitrogen retention capacity (Wang et al., 2025). In this study, the apparent loss load of TN in surface water in 2024 was significantly higher than that in 2023, mainly because the first drainage time in 2024 was earlier, and both drainage volume and TN concentration were higher. This phenomenon reveals that N loss in paddy fields is not only related to water and fertilizer management, but also closely related to rainfall distribution and drainage timing. In actual production, it is necessary to combine climate prediction to optimize drainage timing and reduce N runoff loss.

P has poor mobility in soil, and its loss is mainly dominated by surface water runoff, while the leaching flux in underground seepage water is relatively low (Zhang et al., 2024). The results of this study also confirmed this pattern, as the apparent loss load in surface water was significantly higher than the leaching flux in underground seepage water. Compared with N, the interaction between irrigation regime and straw crushing degree had a more complex effect on P. In this study, the CI had a significant inhibitory effect on P runoff loss in surface water, especially the CI + P, which significantly reduced the apparent loss load of TP in surface water compared with CK, mainly because the CI could reduce surface drainage volume. In addition, the humus formed by the decomposition of powdered straw could combine with P in soil, increasing the retention capacity of soil for P, thereby reducing the dissolution and runoff loss of P (Zhao et al., 2024). The TP leaching flux in underground seepage water showed

significant interannual differences, and was significantly lower in 2024 than in 2023, mainly because the total amount of underground seepage water decreased in 2024. In addition, due to uneven rainfall in 2024, the soil under the CI experienced certain drought stress. Drought stress can inhibit the P mineralization process, aggravate microbial P limitation, and reduce the net generation of leachable P (Li et al., 2024). This further enhanced the inhibitory effect of this treatment on TP leaching, making the decrease of CI compared with CK more significant, indicating that the CI had a better control effect on P leaching in dry years, which provides targeted strategies for P pollution control in paddy fields under different climate conditions.

DOC is the most active component of soil organic matter. It not only participates in the carbon cycle in soil, but also acts as a carrier for N and P migration, affecting the dissolution and adsorption processes of N and P (Guo et al., 2023). In this study, DOC had a stable extremely significant positive correlation with NO_3^--N and TP leaching fluxes, indicating that DOC played an important carrier role in the N and P leaching process. This is consistent with the conclusions of existing studies that DOC can promote the dissolution and migration of N and P (Wang et al., 2021; Fasching et al., 2024). However, the correlation in this study had interannual differences. The correlation between DOC and nitrogen and phosphorus in 2024 was weaker than that in 2023, possibly because the leaching amount of DOC decreased in 2024, leading to a weakened synergistic migration effect between DOC and N and P. Irrigation regime and straw crushing degree synergistically regulated the DOC leaching process, indirectly affecting the migration and loss of N and P. The CI reduced the DOC leaching flux by reducing the total amount of underground seepage water. The DOC leaching flux of powdered straw was significantly lower than that of segmented straw, which is related to the characteristic that powdered straw is more easily decomposed and utilized by microorganisms. Therefore, the DOC leaching flux of CI + P was the lowest in both years.

In summary, irrigation regime dominated the reduction of N and P leaching fluxes by optimizing water management in paddy fields; straw crushing degree mainly regulated the release intensity of carbon, N and P, affecting nutrient availability and migration potential; and DOC as a carrier for the synergistic migration of carbon, N and P, established a close link among the three. The synergistic regulation of the three is the intrinsic mechanism by which CI + P achieves the optimal emission reduction effect.

5. Conclusions

This two-year barrel experiment investigated the effects of irrigation regime (CI vs FSI), straw crushing degree (P vs S), and their interaction on water dynamics, N and P runoff loss in surface water, N and P leaching in seepage water, and DOC migration in paddy fields. The results showed that the CI significantly reduced N and P leaching fluxes by reducing seepage volume and promoting denitrification. Powdered straw was more conducive to reducing the migration and loss of N, P and DOC than segmented straw, and this regulatory effect was significantly affected by climate conditions. DOC was significantly positively correlated with NO_3^--N and TP leaching fluxes, and was a carrier for the

synergistic migration of N and P, its leaching process was synergistically regulated by irrigation regime and straw crushing degree. CI + P was the optimal combination for reducing N and P loss in paddy fields.

Declarations

Author Contribution

Jinhua Zhang: Writing - original draft, Writing - review & editing, Methodology, Visualization. Han Han: Conceptualization, Formal analysis, Methodology, Data curation. Xiaohui Xu: Investigation, Visualization, Validation, Formal analysis. Xiangping Guo: Supervision, Conceptualization, Resources, Writing - review & editing. Jialiang Chen: Formal analysis, Project administration, Funding acquisition, Resources.

Acknowledgments

This study was supported by the Water Conservancy Science and Technology Project of Jiangsu Province (2026019) and the Open Fund Research Project (202601), MNR Field Scientific Observation and Research Station for Land Consolidation and Ecological Protection in Donghai and Yixing, Jiangsu.

References

1. Amin MGM, Akter A, Jahangir MMR, Ahmed T (2021) Leaching and runoff potential of nutrient and water losses in rice field as affected by alternate wetting and drying irrigation. J Environ Manage 297:113402. https://doi.org/10.1016/j.jenvman.2021.113402
2. Bronk DA, Lomas MW, Gilbert PM, Schukert KJ, Sanderson MP (2000) Total dissolved nitrogen analysis: comparisons between the persulfate, UV and high temperature oxidation methods. Mar Chem 69:163–178. https://doi.org/10.1016/S0304-4203(99)00103-6
3. Chen T, Mei Y, Liu X, Zhang Z, Liang Y (2024) Effects of straw at different fermentation phases on soil nutrient availability and microbial activity. Agronomy 14(12):3005. https://doi.org/10.3390/agronomy14123005
4. Chen Y, Du Z, Weng Z, Sun K, Zhang Y, Liu Q, Yang Y, Li Y, Wang Z, Luo Y, Gao B, Chen B, Pan Z, Van Zwieten L (2023) Formation of soil organic carbon pool is regulated by the structure of dissolved organic matter and microbial carbon pump efficacy: A decadal study comparing different carbon management strategies. Glob Chang Biol 29:5445–5459. https://doi.org/10.1111/gcb.16865
5. Cong P, Wang J, Li Y, Liu N, Dong J, Pang H, Zhang L, Gao Z (2020) Changes in soil organic carbon and microbial community under varying straw incorporation strategies[J]. Soil Tillage Res, 2020, 204: 104735. https://doi.org/10.1016/j.still.2020.104735
6. Fasching C, Boodoo KS, Yao H, Rusak JA, Xenopoulos MA (2024) Role of lakes, flood, and low flow events in modifying catchment-scale DOC:TN:TP stoichiometry and export. Water Resour Res 60(3). https://doi.org/10.1029/2023WR034839. e2023WR034839

7. Gbedourorou SK, Tovihoudji PG, Zakari S, Vanclooster M, Akponikpe PBI (2025) Effect of water-saving technologies on nitrogen losses in rice fields: A meta-analysis. Agric Water Manag 312:109400. https://doi.org/10.1016/j.agwat.2025.109400
8. Guo Z, Li P, Yang X, Wang Z, Wu Y, Li G, Liu G, Ritsema CJ, Geissen V, Xue S (2023) Effects of microplastics on the transport of soil dissolved organic matter in the Loess Plateau of China. Environ Sci Technol 57(49):20138–20147. https://doi.org/10.1021/acs.est.3c04023
9. Han H, Fan D, Liu S, Jiang R, Song D, Zou G, He P, Wang M, He W (2025) Integrating straw return and tillage practices to enhance soil organic carbon sequestration in wheat-maize rotation systems in the North China Plain. Agric Ecosyst Environ 384:109555. https://doi.org/10.1016/j.agee.2025.109555
10. Han L, Zhao Y, Peacock CL, Lv H, Feng P, Lin S, Hu K (2025) Mitigating N leaching and N_2O emissions by combining drip irrigation and reduced fertilization with straw incorporation in greenhouse tomato systems. Agric Water Manag 321:109928. https://doi.org/10.1016/j.agwat.2025.109928
11. Huang Q, Zuo Y, Zhu Z, Yang L, Tian Z, Liu G (2024) Exploring the impact of dissolved organic matter on nitrate detection: Developing a lab experiment using standard ultraviolet spectrophotometry. J Chem Educ 101:2030–2038. https://doi.org/10.1021/acs.jchemed.3c00958
12. Huang W, Yu X, Liang H, Wu Y, Xin P, Zhou F (2024) Subsurface fluxes dominate the dissolved nitrogen losses from rice paddies in central China. Agric Ecosyst Environ 363:108881. https://doi.org/10.1016/j.agee.2023.108881
13. Iqbal A, Garnier P, Lashermes G, Recous S (2014) A new equation to simulate the contact between soil and maize residues of different sizes during their decomposition. Biol Fertil Soils 50(4):645–655. https://doi.org/10.1007/s00374-013-0876-5
14. Jiang Y, Liu L, Huang X, Yan Y, Xue R, Ma C, Zhang Q (2025) Mitigating nutrient loss in rice-wheat rotation system: An ecologically engineered solutions with field-ditch-pond systems. Agric Water Manag 322:109956. https://doi.org/10.1016/j.agwat.2025.109956
15. Jin W, Cao W, Liang F, Wen Y, Wang F, Dong Z, Song H (2020) Water management impact on denitrifier community and denitrification activity in a paddy soil at different growth stages of rice. Agric Water Manag 241:106354. https://doi.org/10.1016/j.agwat.2020.106354
16. Kerdraon L, Laval V, Suffert F (2019) Microbiomes and pathogen survival in crop residues, an ecotone between plant and soil. Phytobiomes J 3(4):246–255. https://doi.org/10.1094/PBIOMES-02-19-0010-RVW
17. Li G, Zhang C, Huo Z, Liu Y (2025) Achieving comprehensive water productivity improvement: A multi-objective simulation-optimization model for water productivity-oriented irrigation water management. Agric Water Manag 309:109316. https://doi.org/10.1016/j.agwat.2025.109316
18. Li J, Li Y, Wan Y, Wang B, Waqas MA, Cai W, Guo C, Zhou S, Su R, Qin X, Gao Q, Wilkes A (2018) Combination of modified nitrogen fertilizers and water saving irrigation can reduce greenhouse gas emissions and increase rice yield. Geoderma 315:1–10. https://doi.org/10.1016/j.geoderma.2017.11.033

19. Li N, Li Y, Lou R, Xiong R, Xu H (2023) Adsorption and migration of ammonia nitrogen in sediments in the presence of SiO_2 and HA colloids. Colloids Surf Physicochem Eng Asp 675:132008. https://doi.org/10.1016/j.colsurfa.2023.132008
20. Li P, Sun Y, Hou X (2024) Drought stress impacts soil microbial nutrient limitation more strongly than O_3 pollution. Appl Soil Ecol 201:105496. https://doi.org/10.1016/j.apsoil.2024.105496
21. Liu J, Sævarsson HT, Bechmann M, Krogstad T, Persson T, Øgaard AF (2025) Leaching of dissolved phosphorus and carbon and phosphorus fractionation in drainage: effects of soil type, chemical characteristics and amendments. J Soils Sediments 25:1971–1984. https://doi.org/10.1007/s11368-025-04049-z
22. Murphy J, Riley JP (1962) A modified single solution method for the determination of phosphate in natural waters. Anal Chim Acta 27:31–36. https://doi.org/10.1016/S0003-2670(00)88444-5
23. Park S-I, Yang HI, Park H-J, Seo B-S, Jeong Y-J, Lim S-S, Kwak J-H, Kim H-Y, Yoon K-S, Lee S-M, Choi W-J (2021) Rice straw cover decreases soil erosion and sediment-bound C, N, and P losses but increases dissolved organic C export from upland maize fields as evidenced by $\delta^{13}C$. Sci Total Environ 753:142053. https://doi.org/10.1016/j.scitotenv.2020.142053
24. Qi D, Zhu J, Wang X (2023) Nitrogen loss via runoff and leaching from paddy fields with the proportion of controlled-release urea and conventional urea rates under alternate wetting and drying irrigation. Environ Sci Pollut Res 30:2141–2154. https://doi.org/10.1007/s11356-023-26480-w
25. Shan A, Pan J, Kang KJ, Pan M, Wang G, Wang M, He Z, Yang X (2021) Effects of straw return with N fertilizer reduction on crop yield, plant diseases and pests and potential heavy metal risk in a Chinese rice paddy: A field study of 2 consecutive wheat-rice cycles. Environ Pollut 288:117741. https://doi.org/10.1016/j.envpol.2021.117741
26. Skok A, Bazel Y, Vishnikin A (2023) A new miniaturized microextraction HS-LPME-OIP procedure for ammonium determination based on Nessler‘s method. Chem Pap 77:7303–7309. https://doi.org/10.1007/s11696-023-02903-3
27. Tan X, Shao D, Liu H (2013a) Simulating soil water regime in lowland paddy fields under different water managements using HYDRUS-1D. Agric. Water Manag 132:69–78. http://dx.doi.org/10.1016/j.agwat.2013.10.009
28. Tan X, Shao D, Liu H, Yang F, Xiao C, Yang H (2013b) Effects of alternate wetting and drying irrigation on percolation and nitrogen leaching in paddy fields. Paddy Water Environ 11:381–395. https://doi.org/10.1007/s10333-012-0328-0
29. Tao W, Li J, Li W, Wen C, Gao S, Wang Y, Liu D, Xu L, Jiang Y, Liu Z, Ding Y, Li G (2024) Higher rice productivity and lower paddy nitrogen loss with optimized irrigation and fertilization practices in a rice-upland system. Agric Ecosyst Environ 374:109176. https://doi.org/10.1016/j.agee.2024.109176
30. Tejada M, Benítez C (2014) Effects of crushed maize straw residues on soil biological properties and soil restoration. Land Degrad Dev 25(5):501–509. https://doi.org/10.1002/ldr.2316
31. Wang C, Sardans J, Tong C, Peñuelas J, Wang W (2021) Typhoon-induced increases in porewater nutrient concentrations and CO_2 and CH_4 emissions associated with salinity and carbon intrusion in

a subtropical tidal wetland in China: A mesocosm study. Geoderma 384:114800. https://doi.org/10.1016/j.geoderma.2020.114800

32. Wang X, Guan Y, Jiang X, Li Y, Liu Q, Zhu S, Yan B, Gao J, Wu Q, Zhang W (2025) Effects of ultra-fine rice straw return to the field on water productivity, rice yield and quality in paddy fields on alternating dry and wet conditions. Trans Chin Soc Agric Eng 41(8):97–108. https://doi.org/10.11975/j.issn.1002-6819.202407239
33. Wen S, Cui N, Wang Y, Gong D, Xing L, Wu Z, Zhang Y, Wang Z (2024) Determining effect of fertilization on reactive nitrogen losses through nitrate leaching and key influencing factors in Chinese agricultural systems. Agric Water Manag 303:109055. https://doi.org/10.1016/j.agwat.2024.109055
34. Xia L, Lam SK, Wolf B, Kiese R, Chen D, Butterbach-Bahl K (2018) Trade-offs between soil carbon sequestration and reactive nitrogen losses under straw return in global agroecosystems. Glob Chang Biol 24:5919–5932. https://doi.org/10.1111/gcb.14466
35. Yang Y, Long Y, Li S, Liu X (2023) Straw return decomposition characteristics and effects on soil nutrients and maize yield. Agriculture 13(8):1570. https://doi.org/10.3390/agriculture13081570
36. Zhang H, Lu C, Pang H, Liu N, Zhang X, Li Y (2020) Straw layer burial to alleviate salt stress in silty loam soils: Impacts of straw forms. J Integr Agric 19(1):265–276. https://doi.org/10.1016/S2095-3119(19)62737-1
37. Zhang S, Zhang G, Wang D, Liu Q, Xu M (2021) Investigation into runoff nitrogen loss variations due to different crop residue retention modes and nitrogen fertilizer rates in rice-wheat cropping systems. Agric Water Manag 247:106729. https://doi.org/10.1016/j.agwat.2020.106729
38. Zhang Y, Zhu J, Li C, Peng H, Liu J, Luo Y, Song M, Dai Y, Deng K, Ji X (2025) Optimizing fertilizer application and straw return to fields to minimize nitrogen and phosphorus runoff losses in double-rice cropping systems. Agric Water Manag 317:109601. https://doi.org/10.1016/j.agwat.2025.109601
39. Zhang Y, Zhuang Y, Zhang Q, Zhai L, Zhang L, Wang N, Liu H, Zhuang Y (2024) Multi-site and long-term estimation of phosphorus dynamics for paddy surface water in China based on new MLEpaddy-P. J Environ Manage 369:122267. https://doi.org/10.1016/j.jenvman.2024.122267
40. Zhao Y, Hao Y, Cheng K, Wang L, Dong W, Liu Z, Yang F (2024) Artificial humic acid mediated migration of phosphorus in soil: Experiment and modelling. CATENA 238:107896. https://doi.org/10.1016/j.catena.2024.107896

Figures

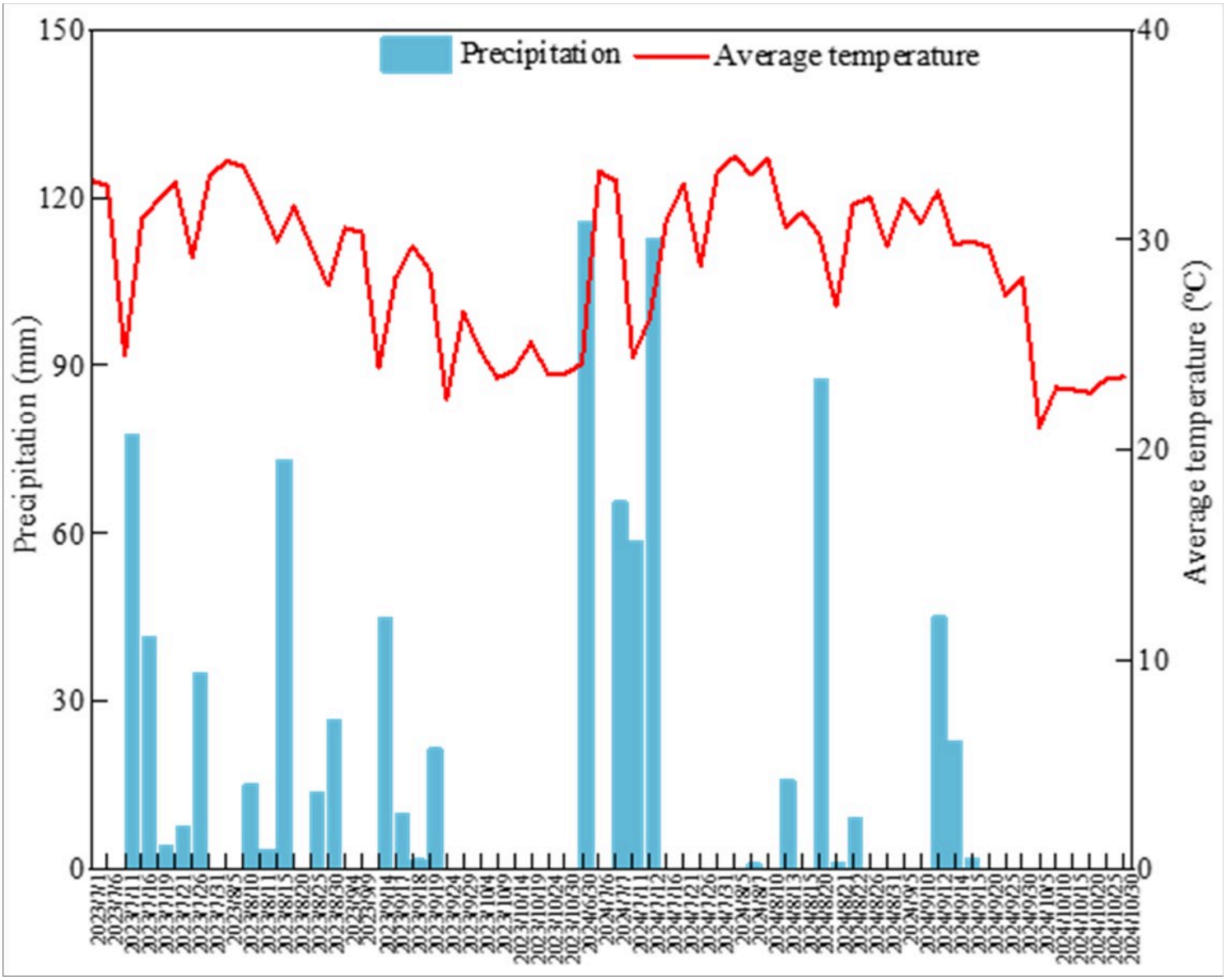


Figure 1

Daily rainfall and mean air temperature over the rice-growing period.

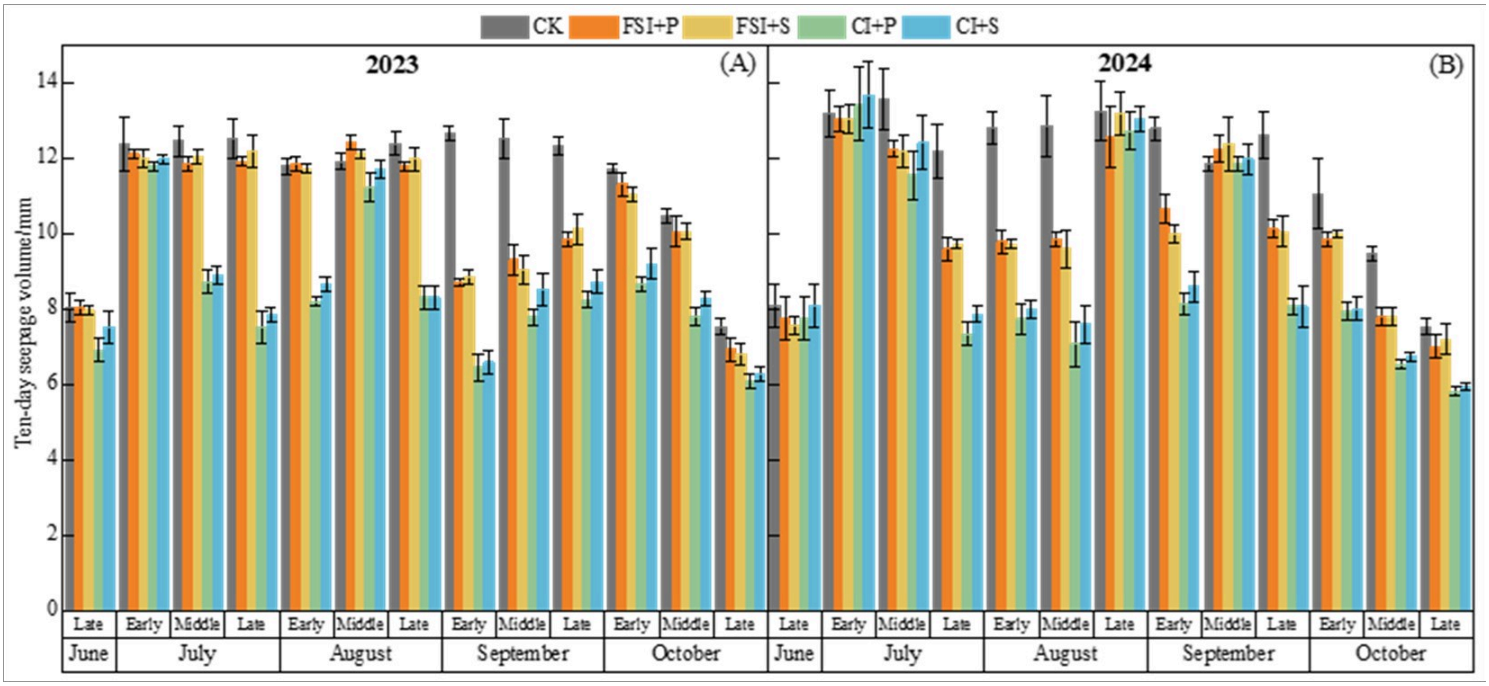


Figure 2

Variation patterns of seepage water volume under different treatments. The x-axis is divided into ten-day periods (early, middle, late) within each month (June, July, August). Error bars denote the standard deviation associated with each mean.

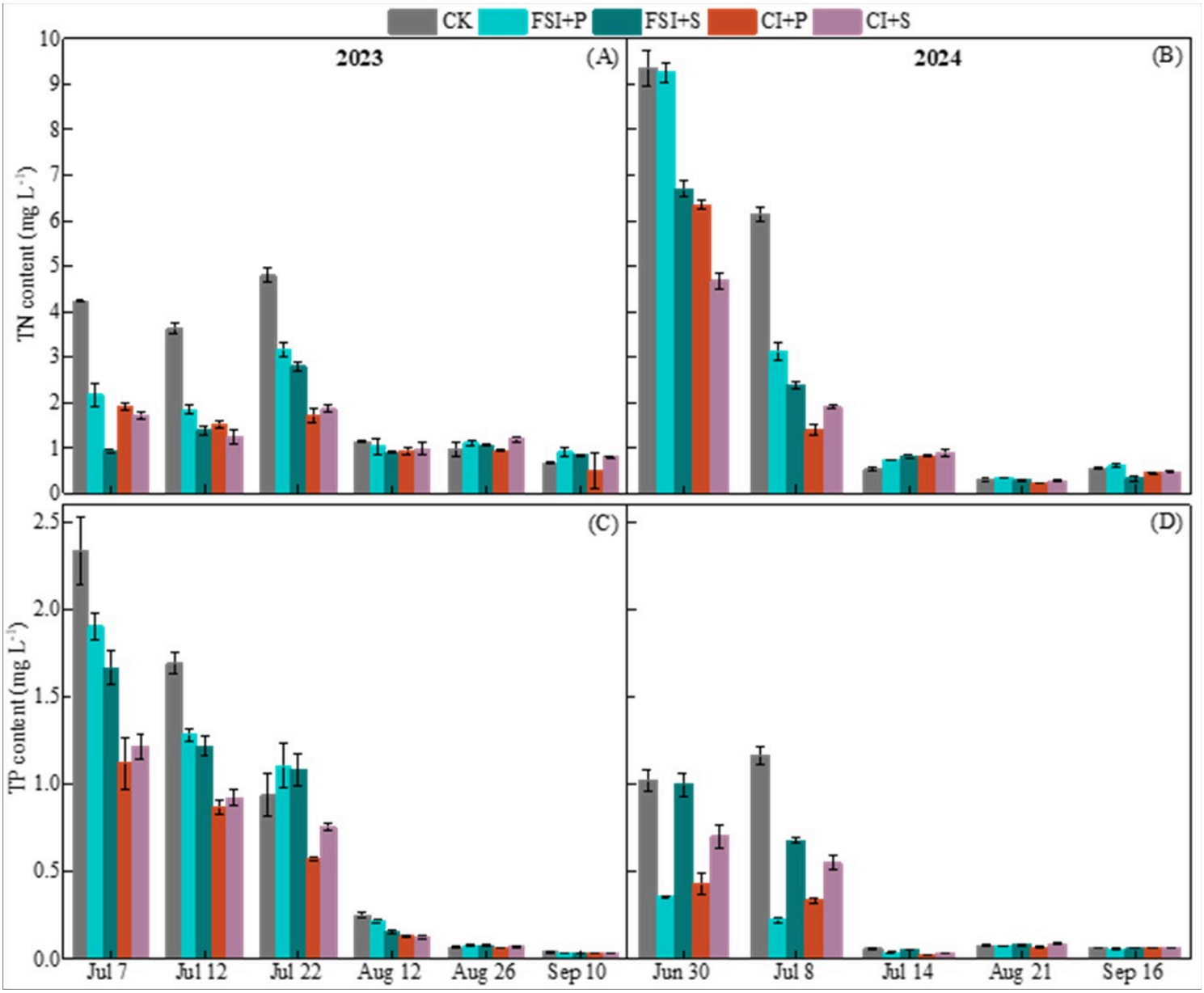


Figure 3

Changes in surface water TN and TP content under different irrigation regimes and straw crushing degrees in 2023 and 2024. Error bars denote the standard deviation associated with each mean.

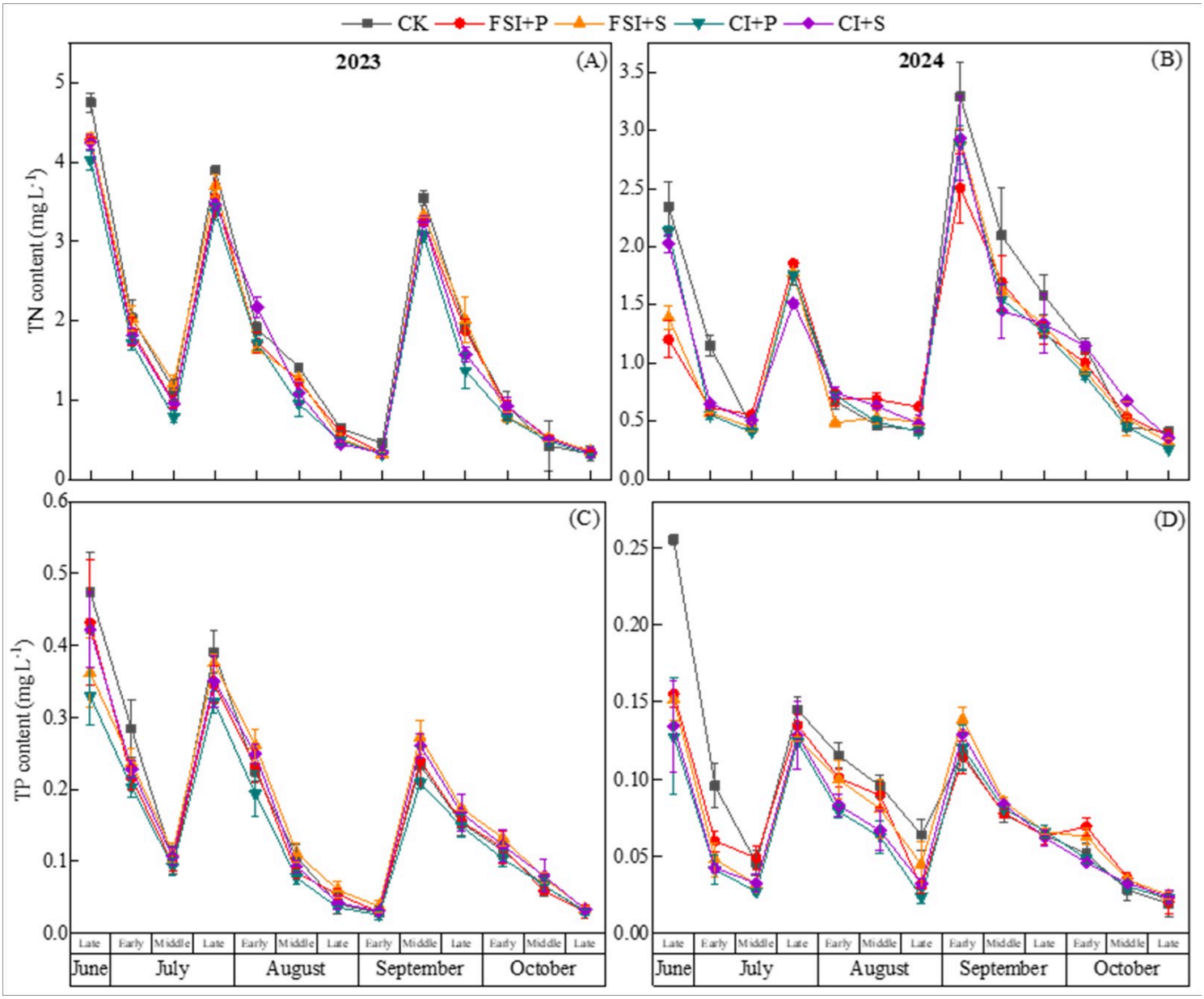


Figure 4

Changes in underground percolating leachate TN and TP content under different irrigation regimes and straw crushing degrees in 2023 and 2024. Error bars denote the standard deviation associated with each mean.

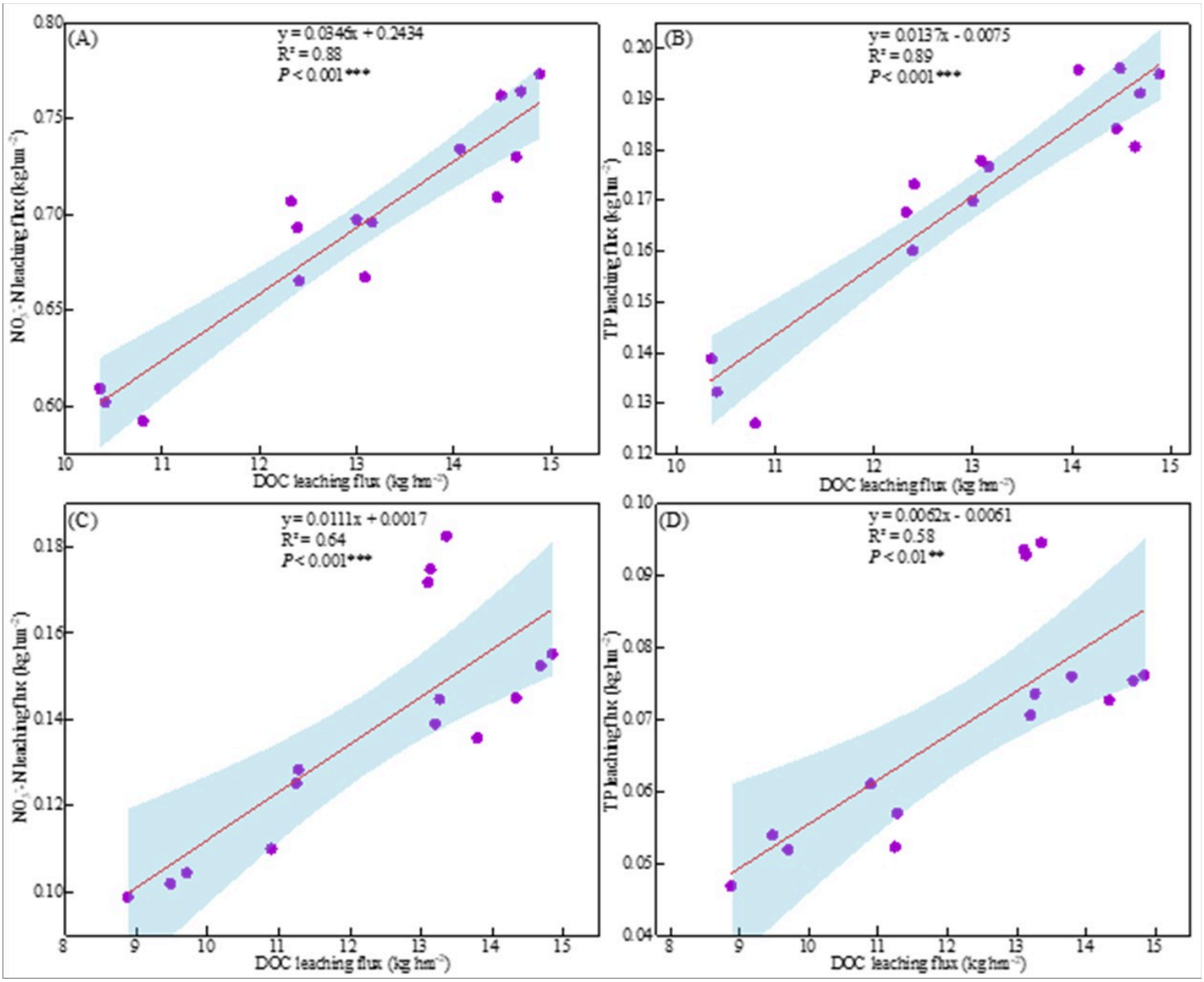


Figure 5

Correlation analysis of DOC with NO_3^--N and TP leaching fluxes. A: NO_3^--N in 2023; B: TP in 2023; C: NO_3^--N in 2024; D: TP in 2024.

Supplementary Files

This is a list of supplementary files associated with this preprint. Click to download.

- SupplementaryMaterial.docx